

Supplemental Materials

Molecular Biology of the Cell

Sluysmans *et al.*

SUPPLEMENTARY MATERIAL

SUPPLEMENTARY FIGURE LEGENDS

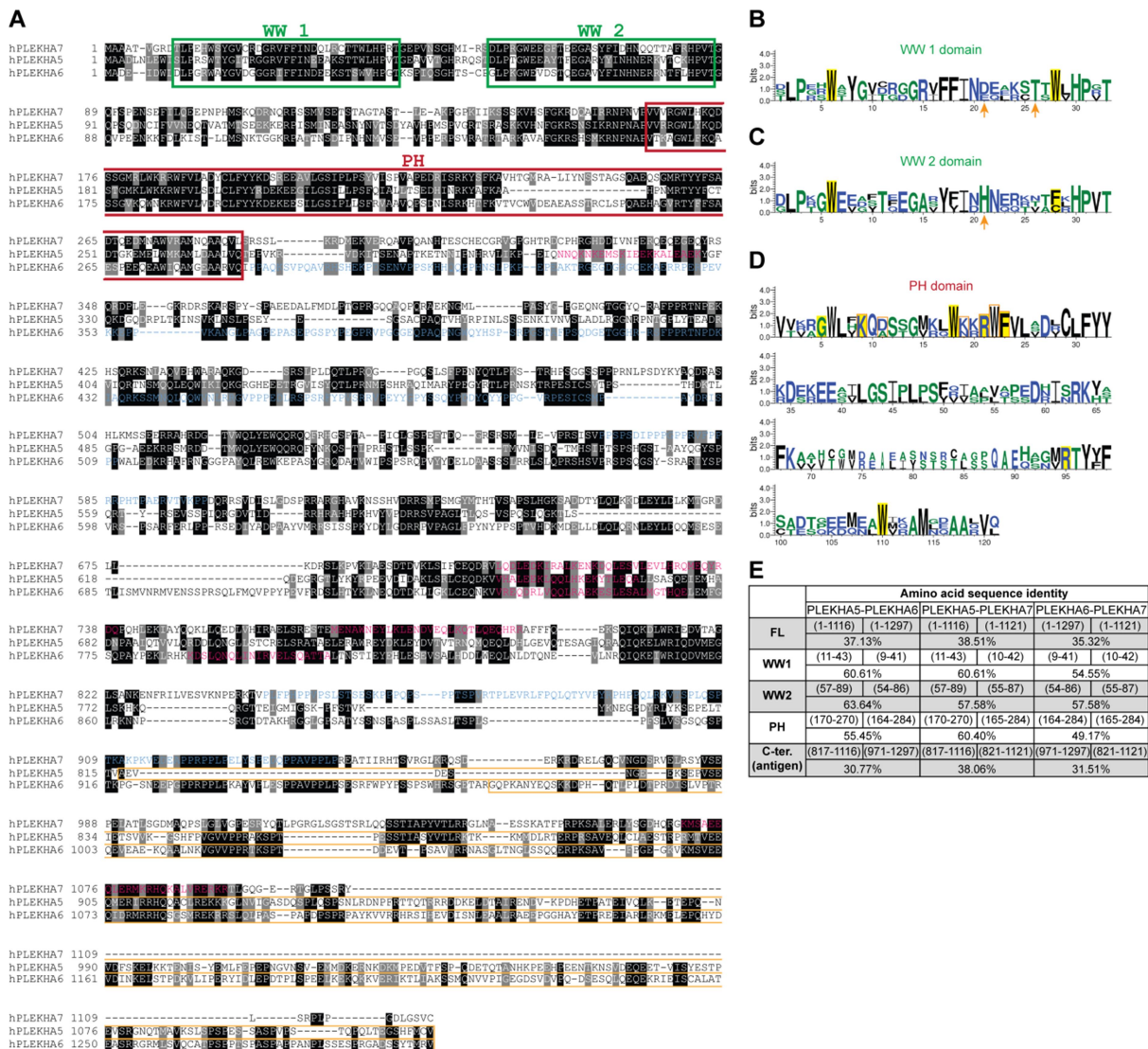


Figure S1

Figure S1. Sequence homology between PLEKHA5, PLEKHA6 and PLEKHA7. (A) Multiple sequence alignment of human PLEKHA5, PLEKHA6 and PLEKHA7 showing identical (black) and similar (grey) residues. WW and PH domains are in green and red boxes, respectively. Residues of coiled-coil and proline-rich domains are indicated in pink and blue, respectively. Orange boxes show regions used as antigens for generation of antibodies. (B-D) Weblogo diagrams of residue conservation in the first (B) and second (C) WW domains, and in the PH domain (D) of human PLEKHA5, PLEKHA6 and PLEKHA7. In B and C, signature residues of the WW domains are highlighted in yellow, and arrows point the amino acids forming the pocket for interaction with PDZD11 (Rouaud *et al.*, 2020). In D, the residues that make up the putative PtdIns(3,4,5)P3-binding motif (PPBM) (Isakoff *et al.*, 1998;

Dowler *et al.*, 2000) are highlighted in yellow, and the key amino acids for the PtdIns(3,4,5)P3 binding PH motif are squared in orange (Jungmichel *et al.*, 2014). (E) Percentage values of amino acid sequence identity between full-length and domains (with indicated amino acid positions) of WW- PLEKHAs.

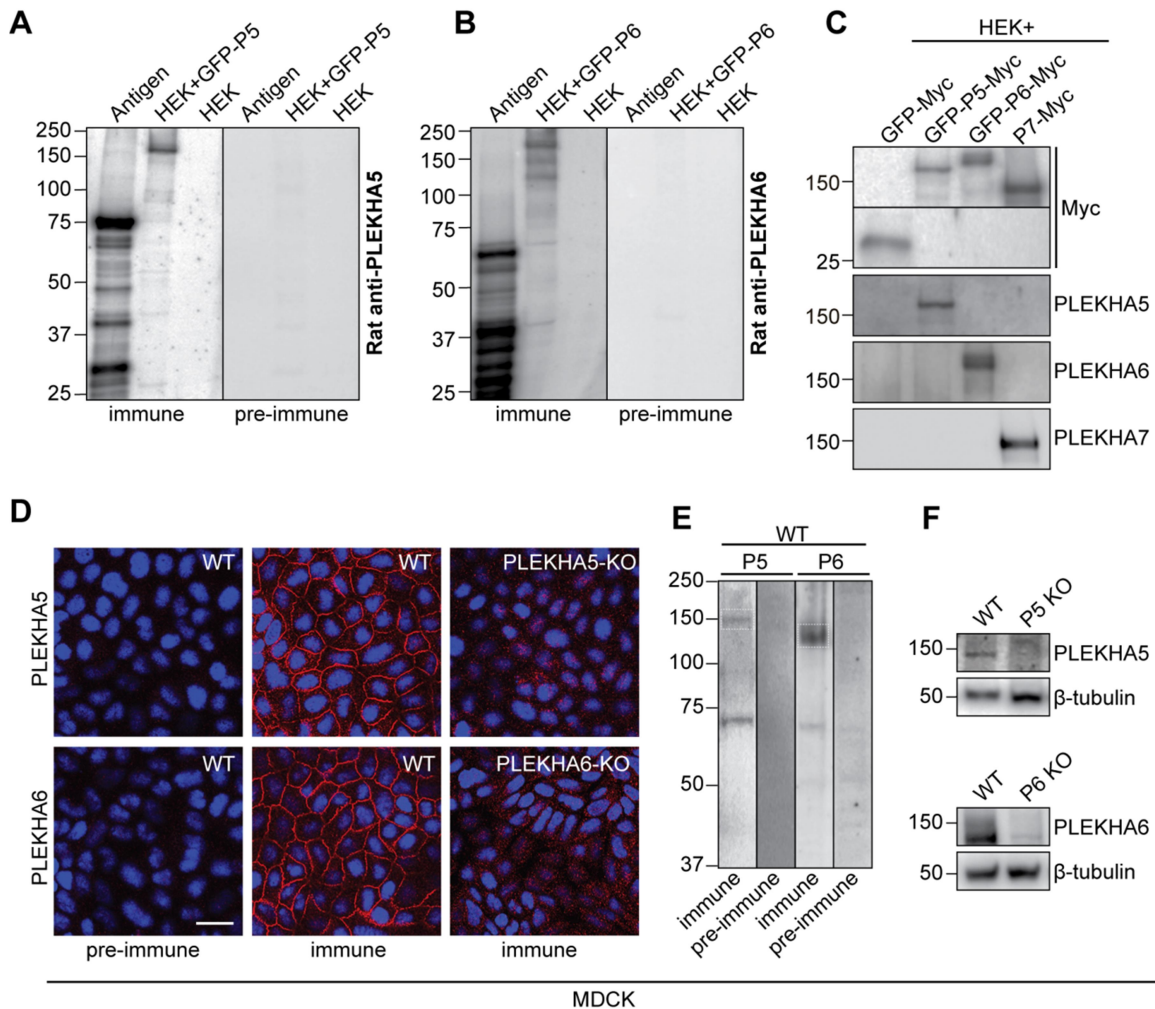


Figure S2

Figure S2. Generation and validation of antibodies against PLEKHA5 and PLEKHA6. (A-B) IB analysis, using anti-PLEKHA5 (A) or anti-PLEKHA6 (B) immune and pre-immune sera, of the respective antigen and of HEK cell lysates expressing the corresponding full-length protein (untransfected HEK lysate as negative control). (C) IB analysis of HEK lysates overexpressing GFP- and Myc-tagged PLEKHA5 (P5), PLEKHA6 (P6) or PLEKHA7 (P7) (GFP-Myc as control), using anti-PLEKHA5, -PLEKHA6 and -PLEKHA7 (-Myc as loading control) antibodies, showing the absence of cross-reaction. (D-F) IF microscopy (D) and IB analysis (E-F) of WT and KO MDCK cells (see Figure S4 for KO lines), using anti-PLEKHA5 (P5) or anti-PLEKHA6 (P6) immune and pre-immune sera. Bar= 20 μ m. β -tubulin serves as loading control.

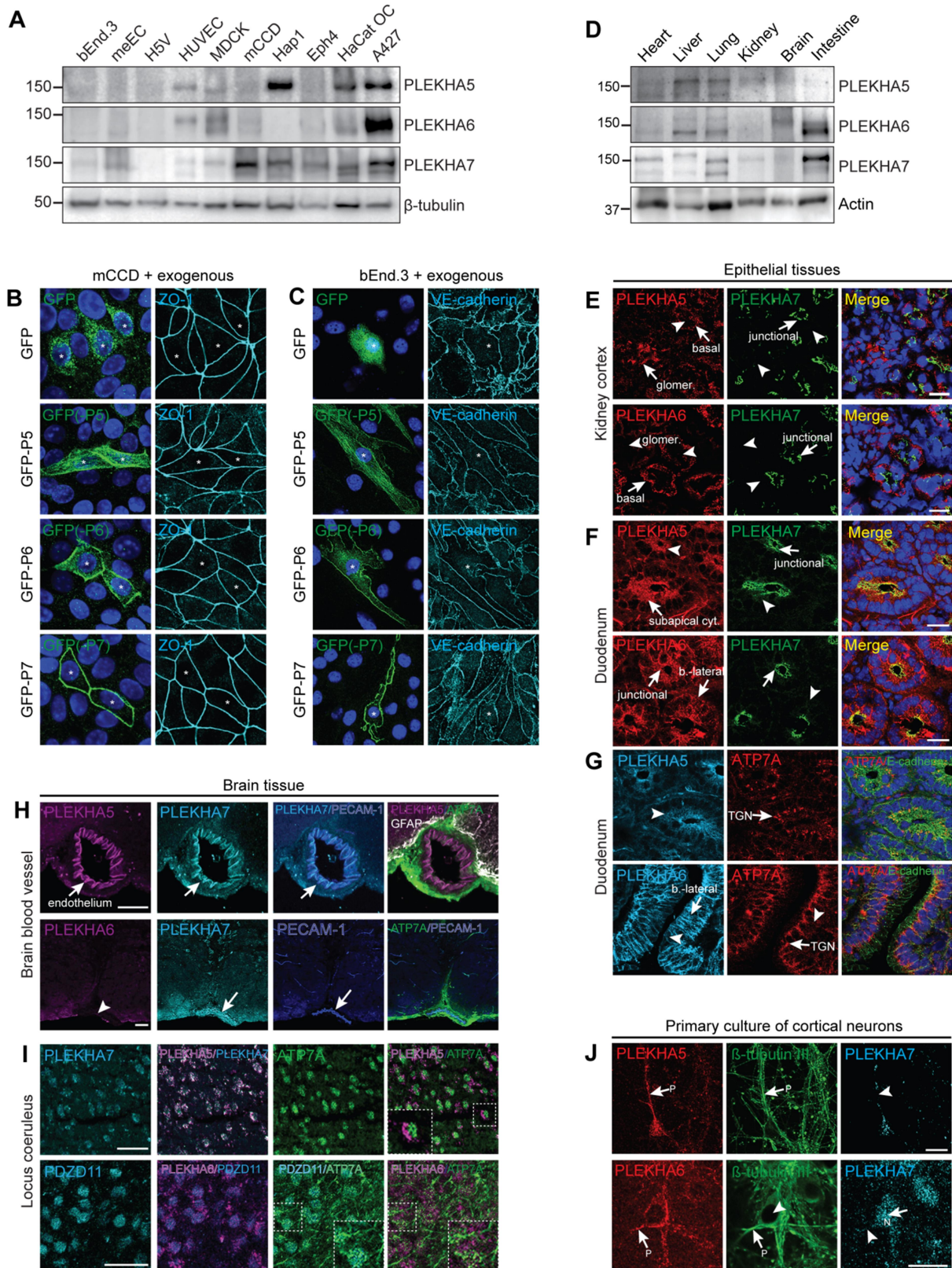


Figure S3

Figure S3. Expression and localization of PLEKHA5, PLEKHA6 and PLEKHA7 in tissues and cells. (A, D) IB analysis of PLEKHA5, PLEKHA6 and PLEKHA7 (with either β -tubulin or actin as loading controls) in lysates of the indicated cell types (A) and mouse tissues (D). (B, C) IF microscopy analysis of GFP-tagged exogenously expressed PLEKHA5 (P5), PLEKHA6 (P6) and PLEKHA7 (P7) (GFP as control) either in epithelial mCCD (B) or endothelial bEnd.3 cells (C). Asterisks show transfected cells. (E-G) IF microscopy analysis of the localization of WW-PLEKHAs and ATP7A (indicated in each panel) in sections of mouse kidney cortex (E) and duodenum (F, G). Basal, baso-lateral (b.-lateral), junctional, glomerular (glomer.), sub-apical cytoplasmic (sub-apical cyt.) or trans-Golgi network (TGN) labeling is indicated by arrows. Arrowheads indicate low/undetectable labeling. Bars= 20 μ m. (H-I) IF microscopy of mouse brain sections focusing on blood vessels (PECAM-1 as endothelial marker (blood vessels)) (H) or locus coeruleus (I). All WW-PLEKHAs and PDZD11 are expressed in neurons in locus coeruleus region, and ATP7A expression in locus coeruleus neurons appears as puncta. Bars= 50 μ m. (J) IF microscopy analysis of WW-PLEKHAs in primary cultures of cortical neurons, co-labeled with anti- β -tubulin III to identify neuronal projections (pointed with P). N shows nucleus, arrows indicate labeling, arrowheads indicate low/undetectable labeling. Bars= 20 μ m.

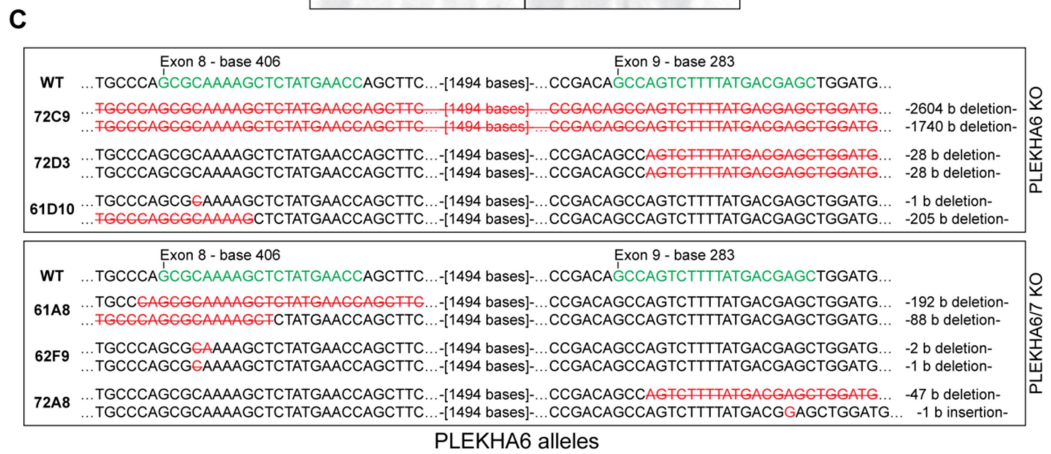
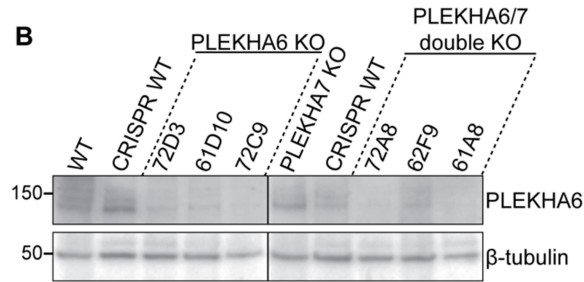
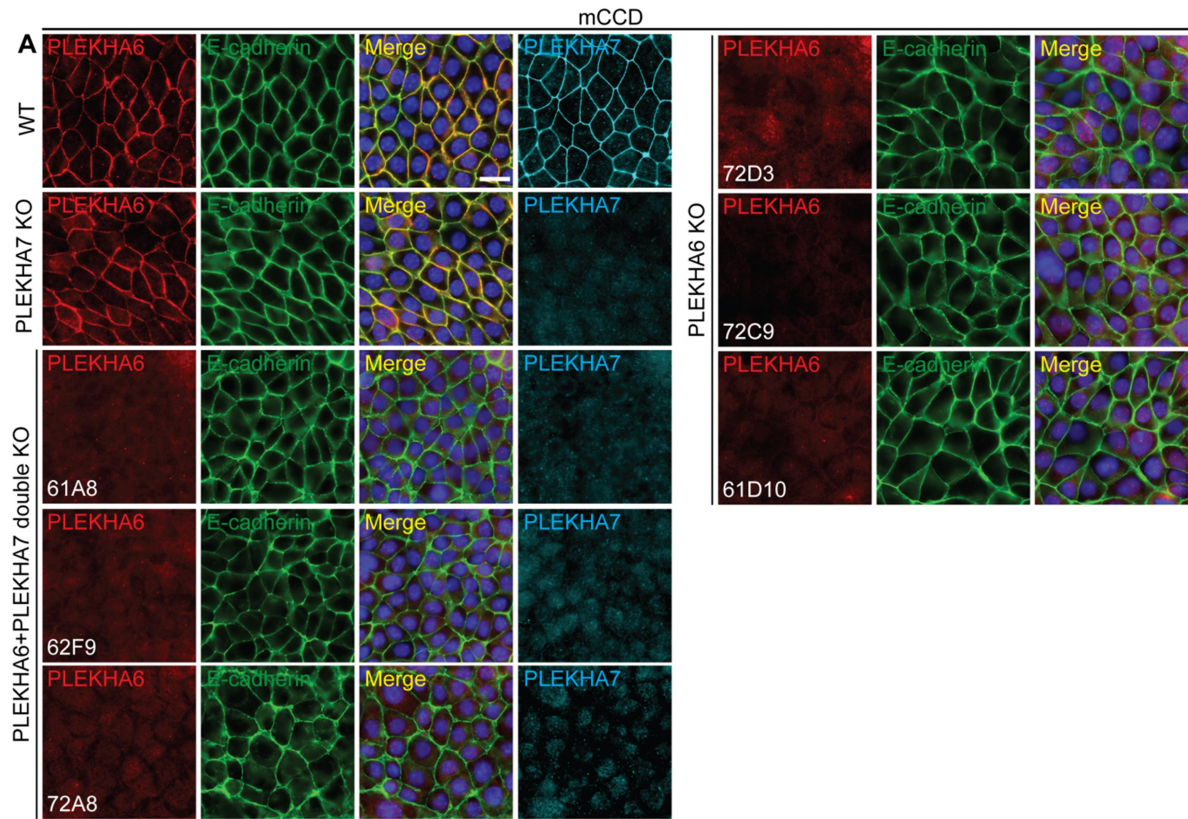
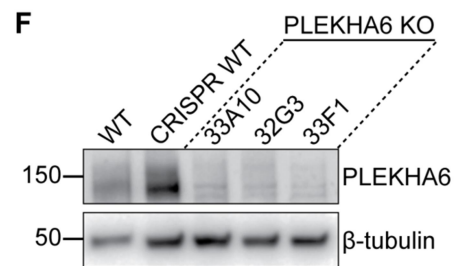
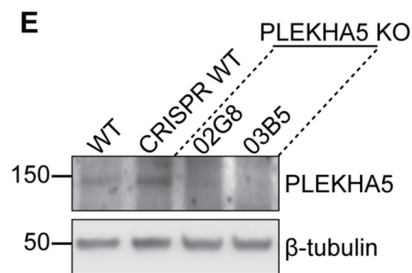
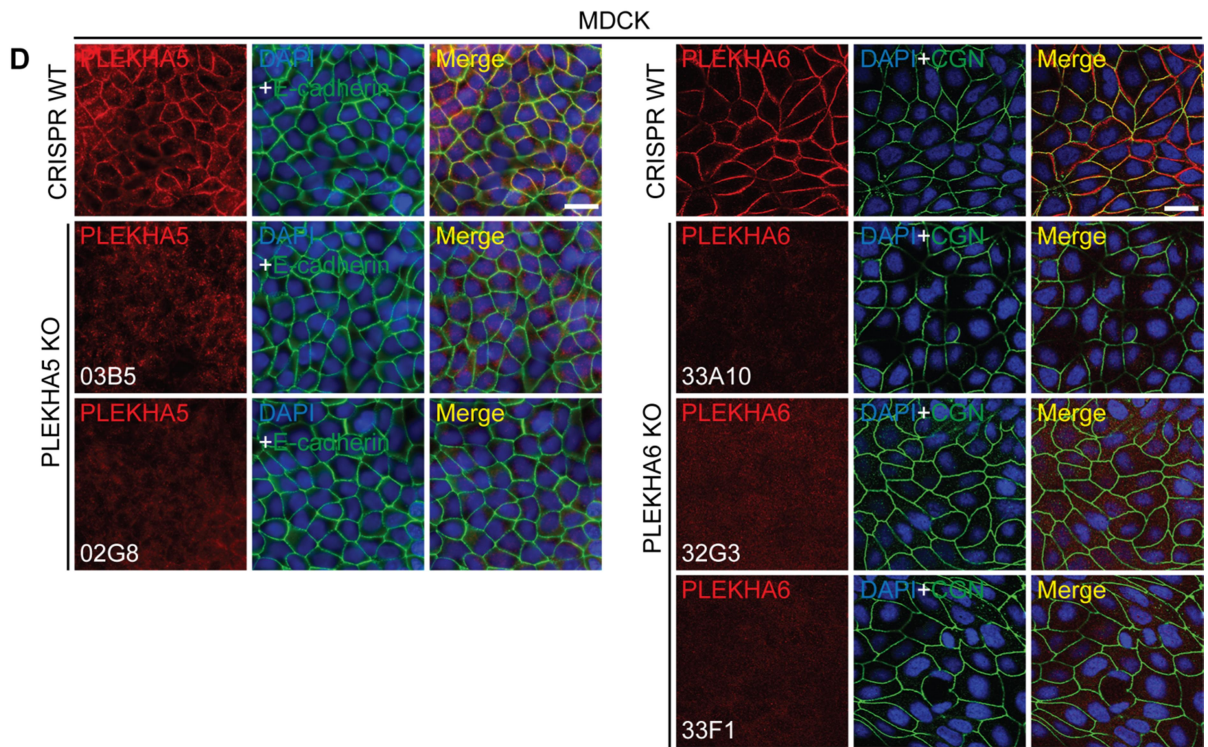


Figure S4-1



G

PLEKHA6 alleles

	Exon 11 - base 111		
WTGAACCAGCTC	ATCAACATTCGGGTGGAGCTGTCCC...	
33A10GAACCAGCTC CG -[135b]-TCTTCAGTTC	ATCAACATTCGGGTGGAGCTGTCCC... ATCAACATTCGGGTGGAGCTGTCCC...	-2 b deletion- -143 b insertion-
32G3GAACCAGCTCTC-[108b]-GC	ATCAACATTCGGGTGGAGCTGTCCC...	-112 b insertion-
GAACCAGCTCTC-[108b]-GC	ATCAACATTCGGGTGGAGCTGTCCC...	-112 b insertion-
33F1GAACCAGCTCC-[34b]-TC	ATCAACATTCGGGTGGAGCTGTCCC...	-38 b insertion-
GAACCAGCTCC-[34b]-TC	ATCAACATTCGGGTGGAGCTGTCCC...	-38 b insertion-

PLEKHA6 KO

Figure S4-2

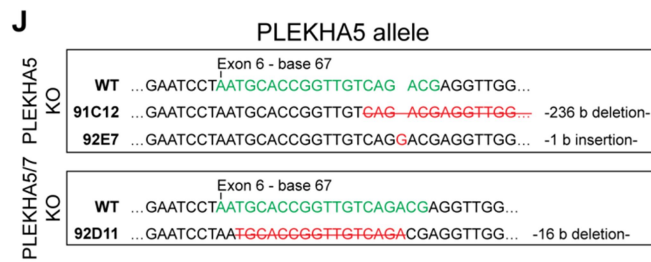
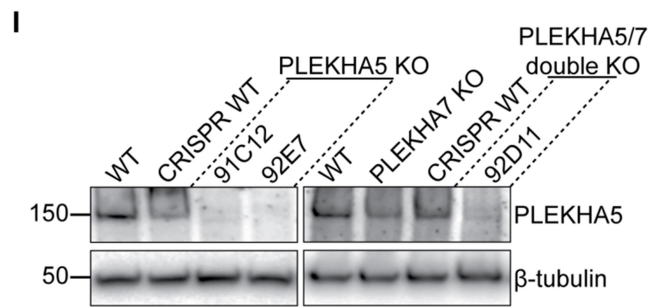
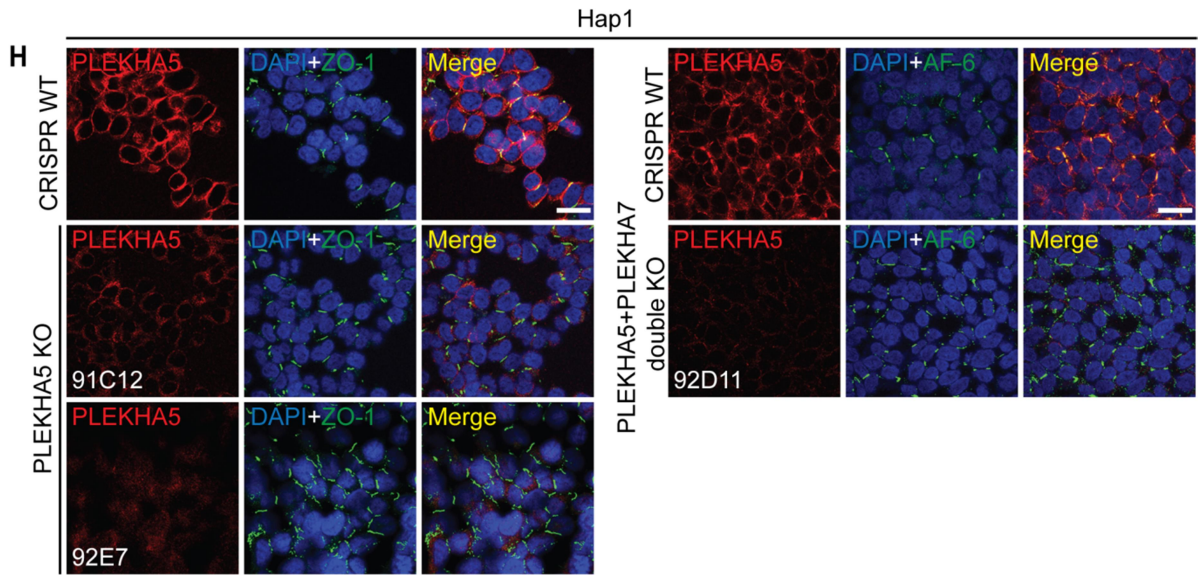


Figure S4-3

Figure S4. Generation of single and double PLEKHA5, PLEKHA6 and PLEKHA7 knock-out cell lines.

(A-C) Validation of CRISPR/Cas9-mediated deletion of PLEKHA6 in mCCD (either WT or PLEKHA7 KO background) by IF (A) and IB (B) analysis, and by genomic sequencing (C). E-cadherin is used as a junctional and lateral marker for internal reference in IF analysis. (D-G) Validation of CRISPR/Cas9-mediated deletion of either PLEKHA5 or PLEKHA6 in MDCK by IF microscopy (D) and IB (E, F) analysis and genotyping (G). Since full genomic sequence for dog PLEKHA5 is not available alleles for MDCK PLEKHA5 KO clones could not be genotyped. (H-J) Validation of CRISPR/Cas9-mediated deletion of PLEKHA5 in Hap1 (either WT or PLEKHA7 KO background) by IF microscopy (H) and IB (I) analysis, and by sequencing (J). Bars= 20 μ m. In C, G and J, CRISPR targets are depicted in green in the WT sequences, with their position in the exon, and respective indels in the alleles of the KO clones obtained are indicated in red.

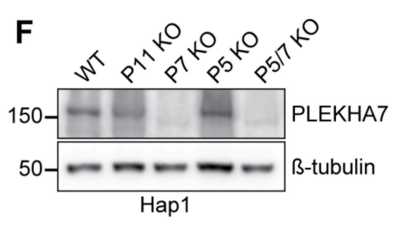
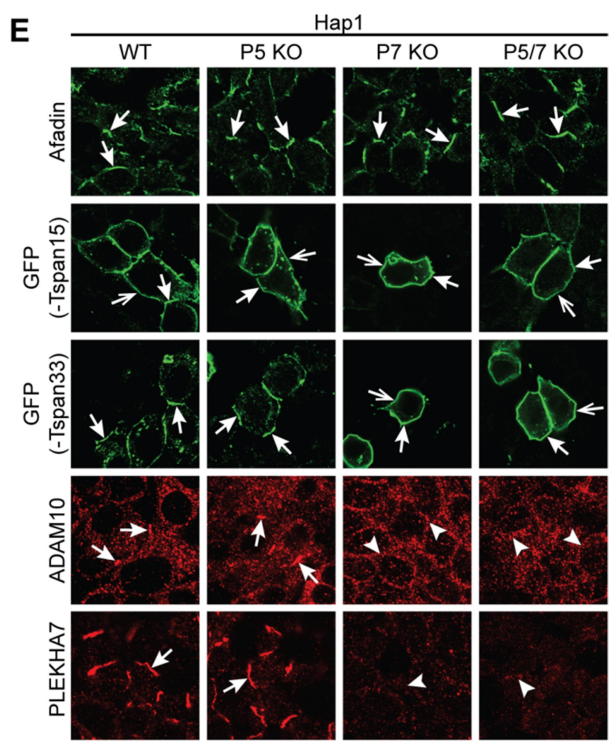
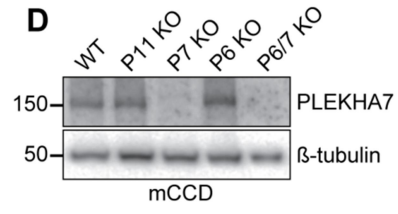
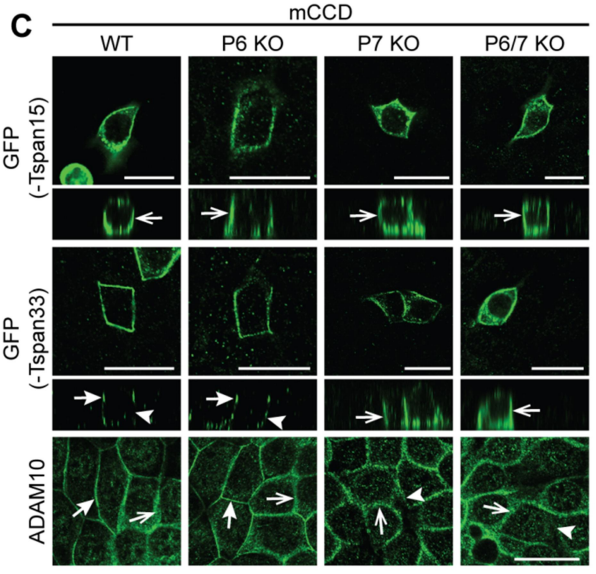
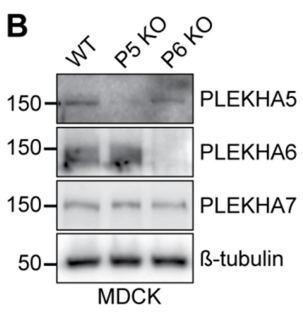
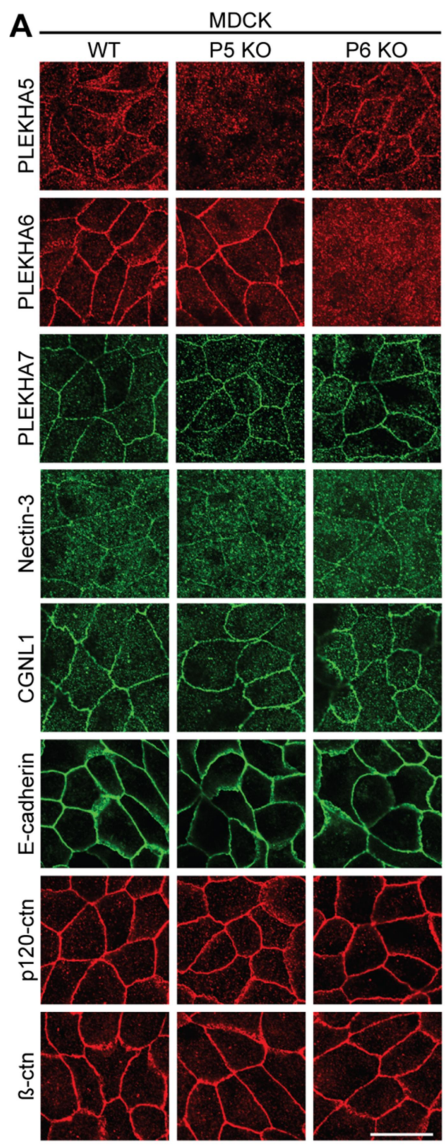


Figure S5

Figure S5. Knock-out of PLEKHA5 or PLEKHA6 does not affect the localization of cadherin complex proteins, Tspan15, Tspan33, ADAM10 and PLEKHA7. (A,C,E). IF microscopy analysis of the localizations of endogenous WW-PLEKHAs (A,E), nectin-3, paracingulin (CGNL1), E-cadherin, p120-catenin (ctn) and β -ctn (A), ADAM10 (C,E), afadin (E) and the exogenous TspanC8s Tspan33 and Tspan15 (C,E) in MDCK (A), mCCD (C) and Hap1 (E) WT and KO cells. Genotypes of KO cells are indicated on top of each column: P5=PLEKHA5, P6=PLEKHA6, P7=PLEKHA7. The phenotype of PDZD11-KO cells is identical to the phenotype of PLEKHA7-KO cells (Shah *et al.*, 2018). Images showing Z section (taken at the horizontal middle position of XY view) were from cells grown on Transwells. Arrows indicate labeling, arrowheads indicate low/undetectable labeling. Bars= 20 μ m. (B, D, F) IB analysis of the expression of WW-PLEKHAs in WT and KO cells: MDCK (B), mCCD (D) and Hap1 (F).

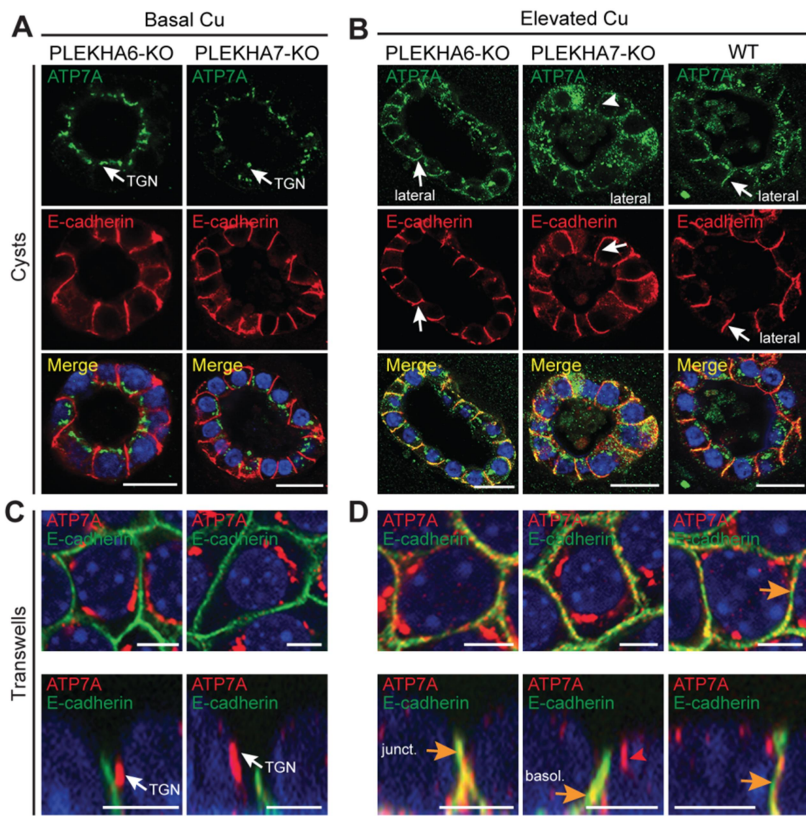


Figure S6-1

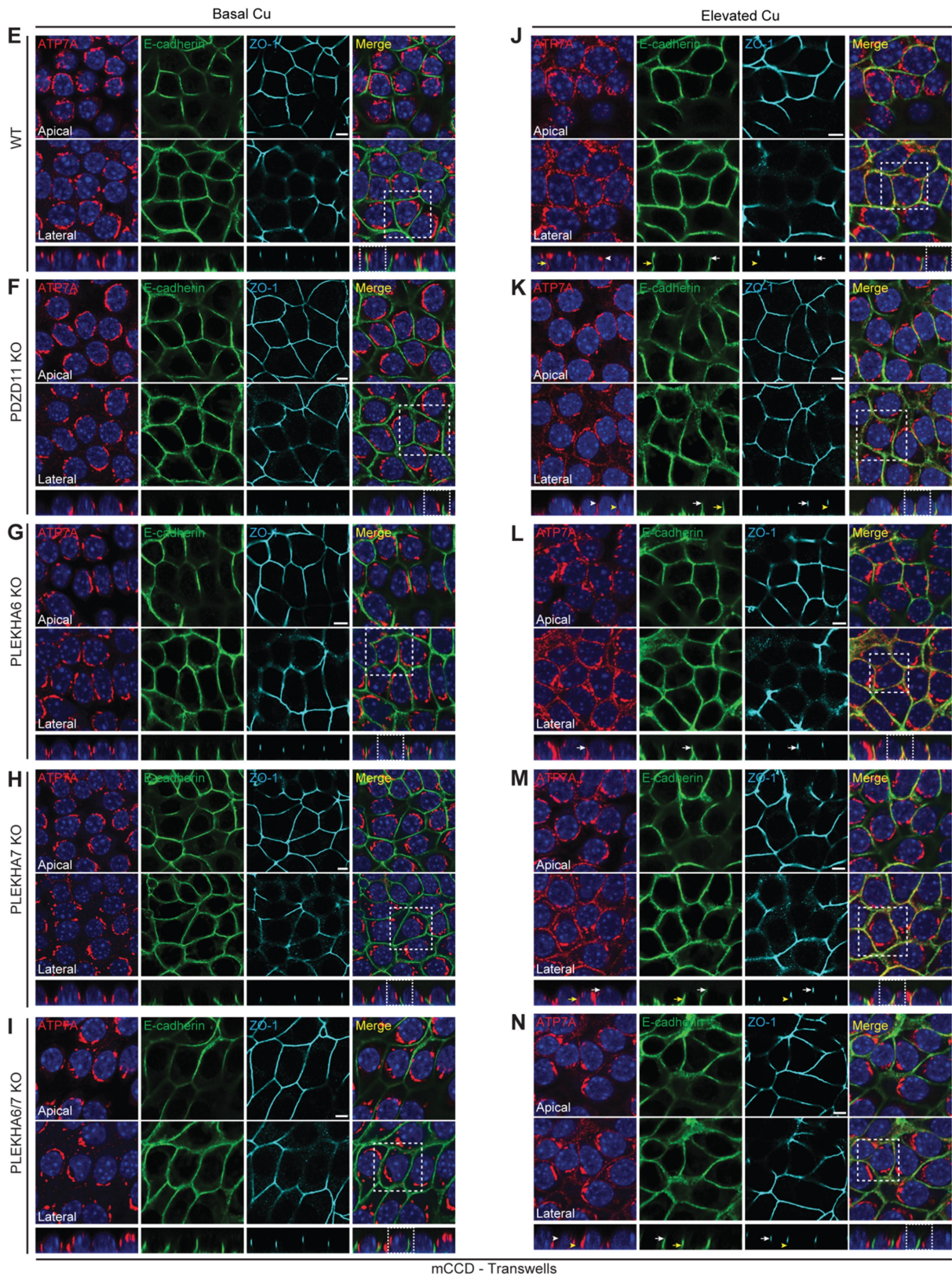
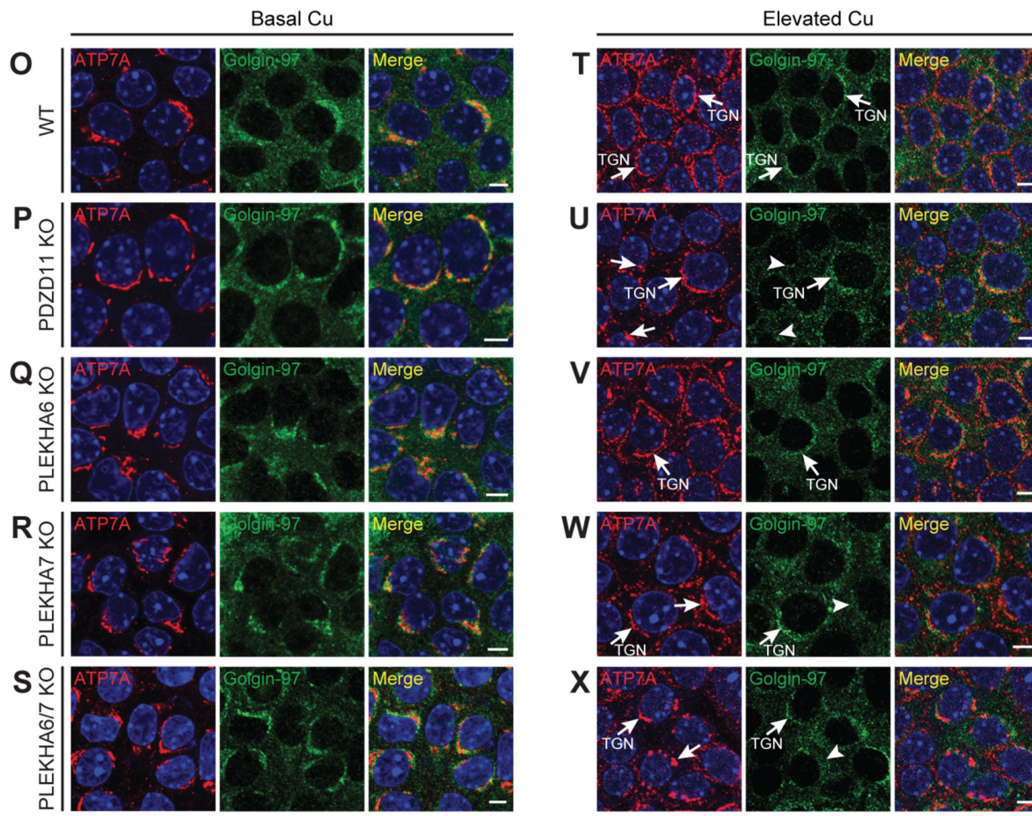


Figure S6-2



mCCD - Transwells

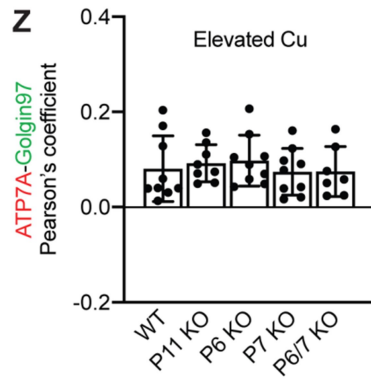
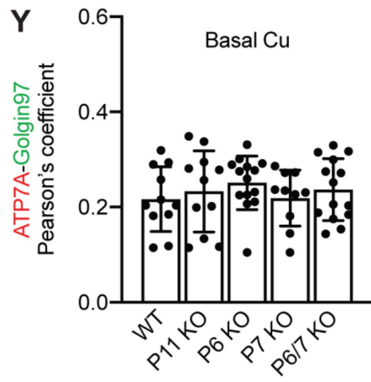


Figure S6-3

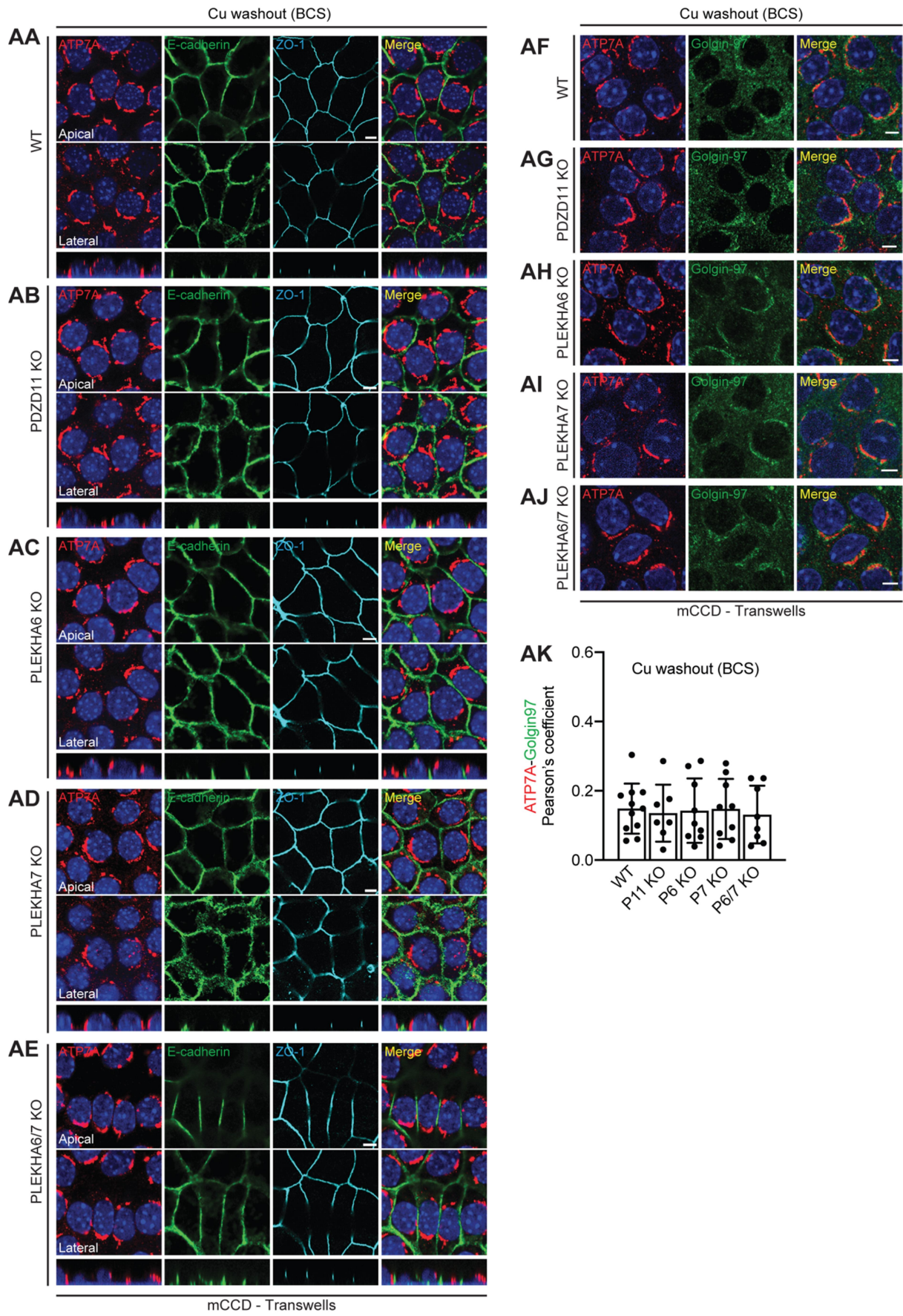


Figure S6-4

Figure S6. Effect of KO of PDZD11 and of either single or double KO of PLEKHA6 and PLEKHA7 on the localization of ATP7A in mCCD cells. (A-D) IF microscopy analysis of the localization of ATP7A in either PLEKHA6-KO or PLEKHA7-KO mCCD cysts (A-B) and monolayers polarized on Transwells (C-D) either under basal copper conditions (A, C) or in elevated copper (B, D). TGN= trans-Golgi network. Lateral, apical and basal ATP7A labeling in elevated copper are indicated by arrows (B). Arrowheads indicate low/undetectable labeling. Orange arrows and red arrowheads in D indicate ATP7A labeling colocalized and non-colocalized with E-cadherin, respectively. Bars= 20 μm (A-B), 5 μm (C-D). (E-N) IF microscopy analysis of the localization of ATP7A in polarized monolayers of mCCD cells (E, J=WT; F,K=PDZD11-KO; G,L=PLEKHA6-KO; H,M=PLEKHA7-KO; I,N=PLEKHA6-PLEKHA7 double KO) grown on Transwells under basal (E-I) or elevated (J-N) copper conditions. Dotted white squares/rectangles indicate high magnification areas shown in Figure 3 and in Figure S6C-D. (O-X) IF microscopy analysis of the localization of ATP7A and golgin-97 in polarized monolayers of mCCD cells (O, T=WT; P, U=PDZD11-KO; Q, V=PLEKHA6-KO; R, W=PLEKHA7-KO; S, X=PLEKHA6-PLEKHA7 double KO) grown on Transwells under basal (O-S) or elevated (T-X) copper conditions. (Y-Z) Quantification of the colocalization of ATP7A and golgin-97 using Pearson's correlation coefficient under either basal Cu (Y) or elevated Cu (Z). Dots show replicates corresponding to individual images from 3 independent experiments (n=10-14). Bars represent mean \pm SD and show no significant difference between WT and KO cells. (AA-AE) IF microscopy analysis of the localization of ATP7A in polarized monolayers of mCCD cells (AA=WT; AB=PDZD11-KO; AC=PLEKHA6-KO; AD=PLEKHA7-KO; AE=PLEKHA6-PLEKHA7 double KO) grown on Transwells treated with CuCl_2 before copper washout (BCS chelation). (AF-AJ) IF microscopy analysis of the localization of ATP7A and golgin-97 in polarized monolayers of mCCD cells (AF=WT; AG=PDZD11-KO; AH=PLEKHA6-KO; AI=PLEKHA7-KO; AJ=PLEKHA6-PLEKHA7 double KO) grown on Transwells treated with CuCl_2 before copper washout (BCS chelation). (AK) Quantification of the colocalization of ATP7A and golgin-97 using Pearson's correlation coefficient in cells grown on Transwells treated with CuCl_2 before copper washout (BCS chelation). Dots show replicates corresponding to individual images from 3 independent experiments (n=7-9). Bars represent mean \pm SD and show no significant difference between WT and KO cells. For XY analysis (E-N, AA-AE), a more apical and a more basal plane of focus were imaged, using ZO-1 and E-cadherin as markers for apical junctions and lateral contacts, respectively. Merge images show colocalization between either E-cadherin and ATP7A (A-N, AA-AE) or golgin-97 and ATP7A (O-X, AF-AJ). ATP7A labeling is detected in the TGN in all cells in basal Cu conditions and is targeted to different degrees to the cell periphery in KO cells. Copper washout resulted in the return of ATP7A to the Golgi in all cells. Bars= 5 μm .

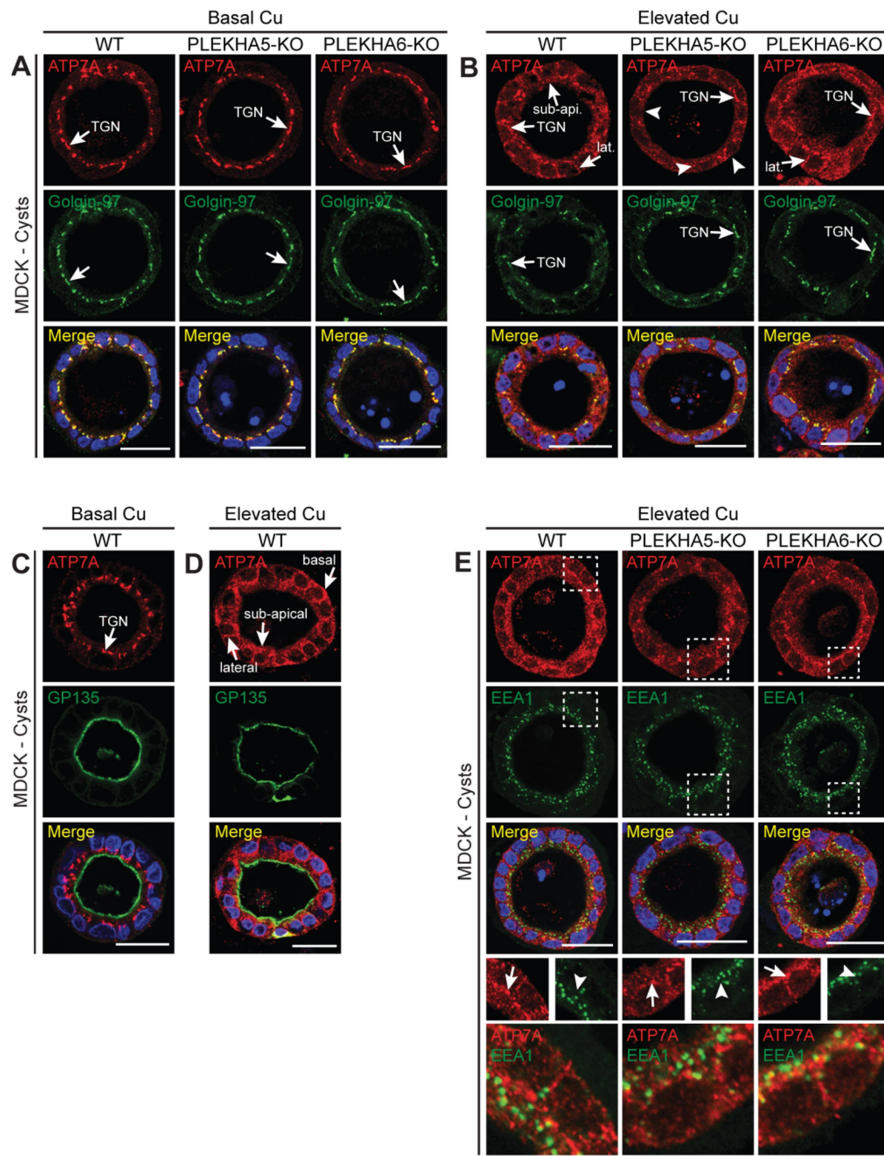


Figure S7-1

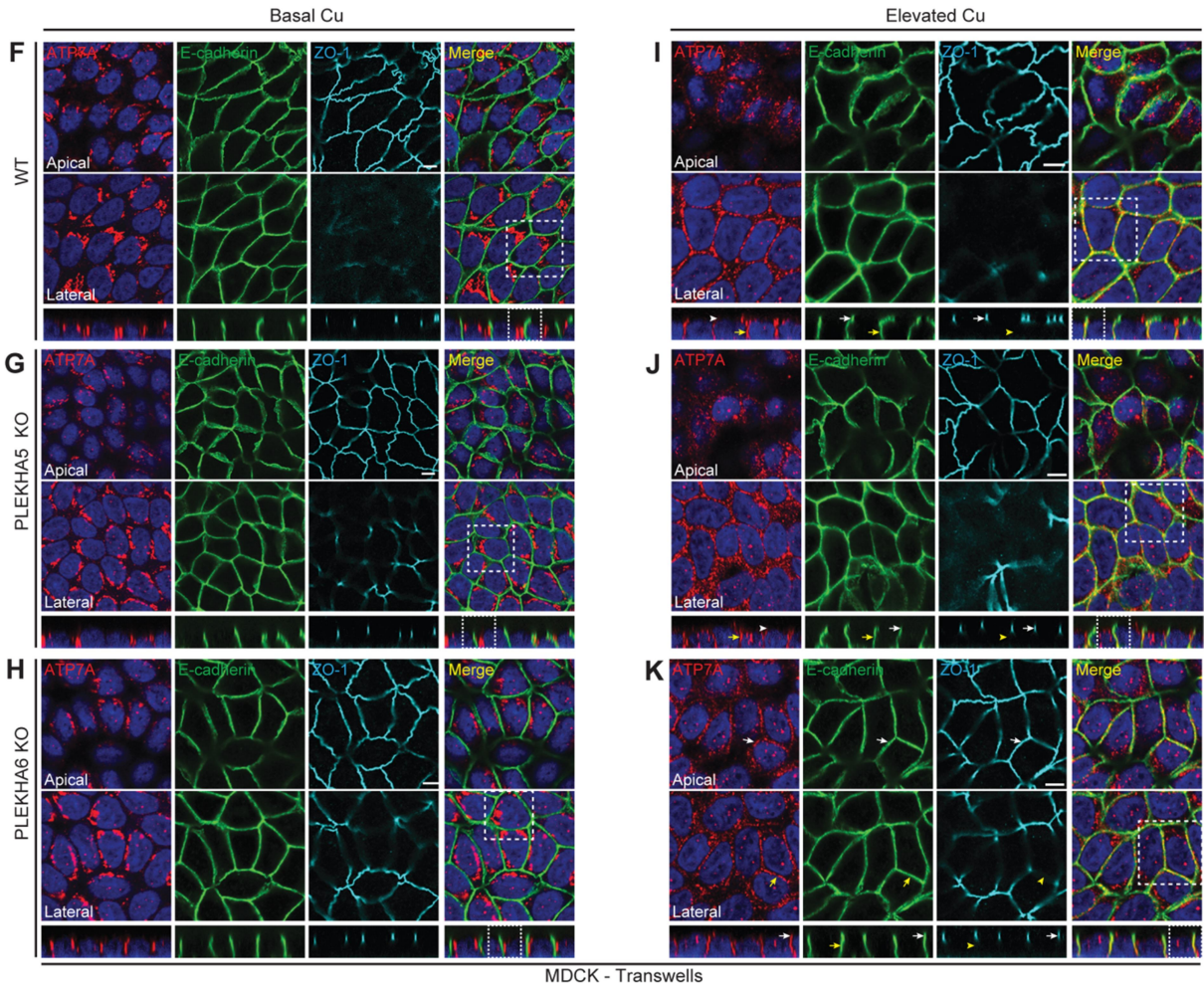


Figure S7-2

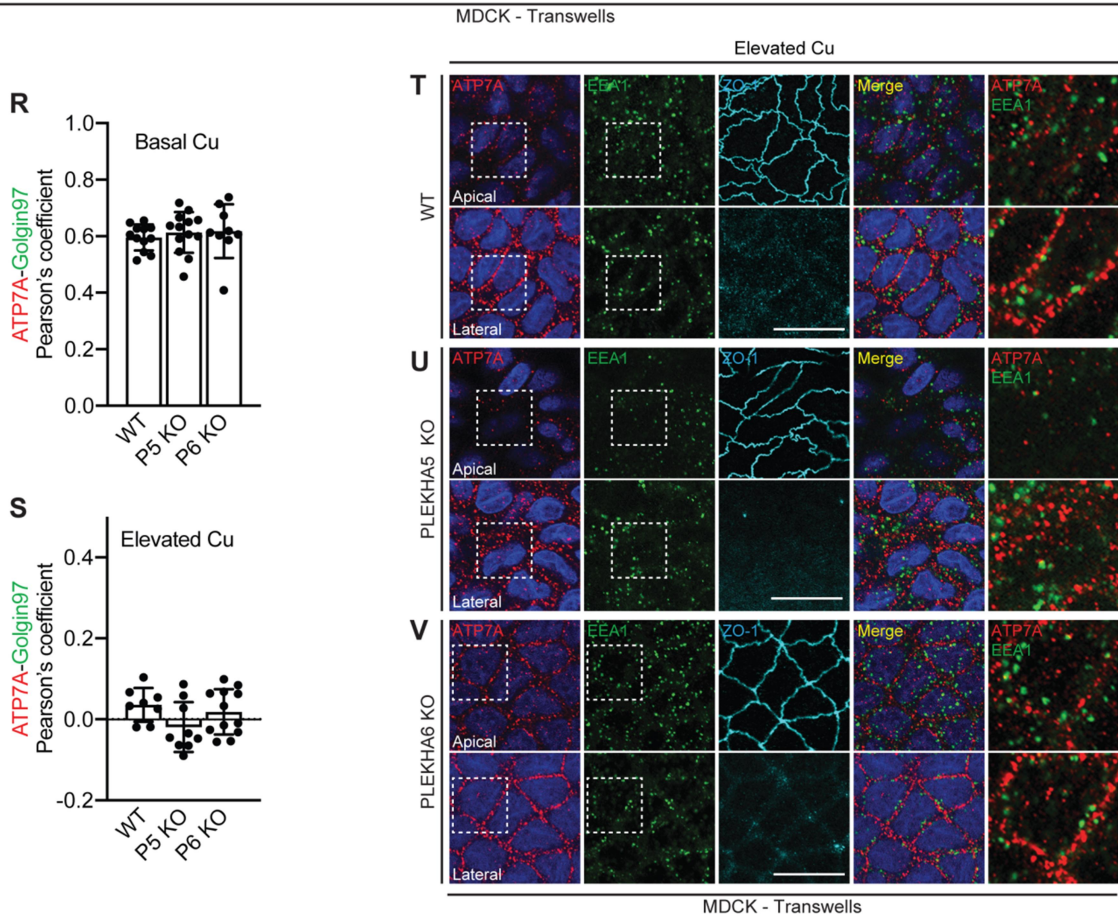
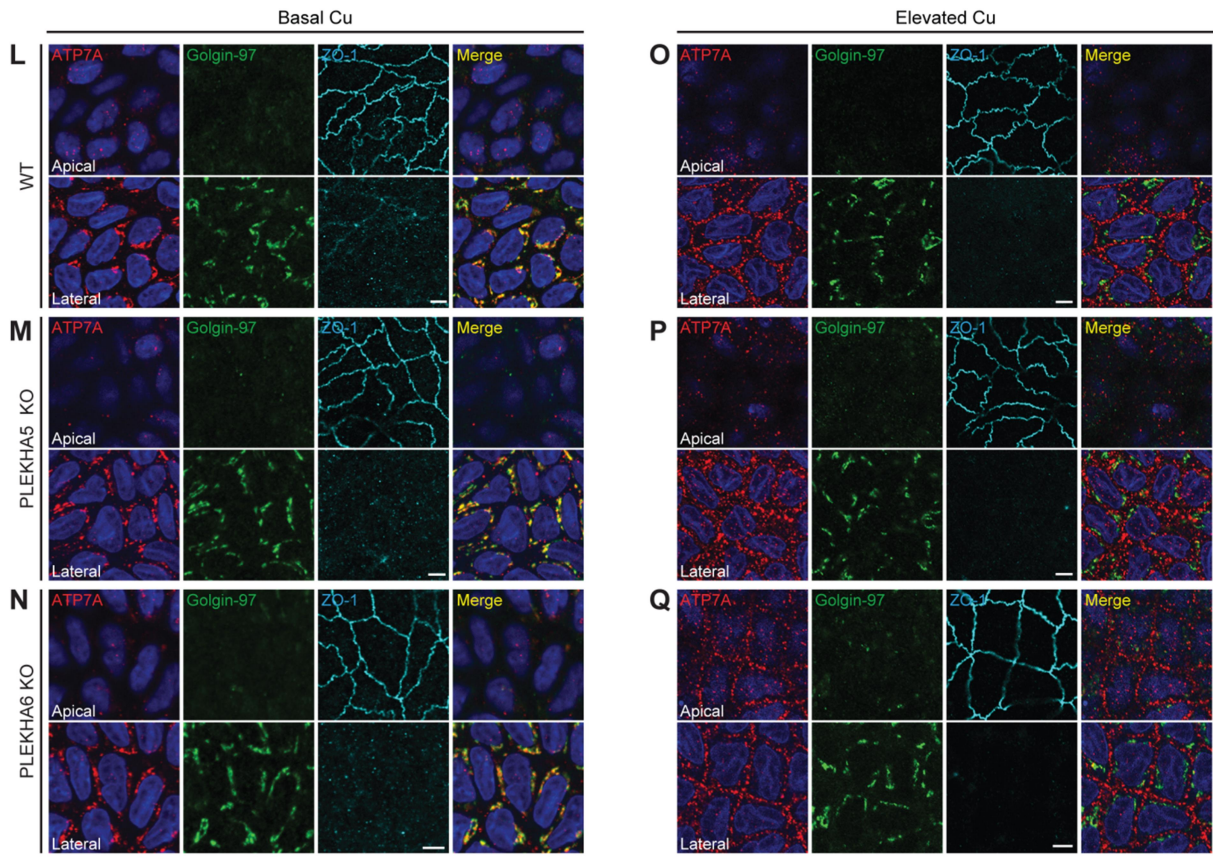


Figure S7-3

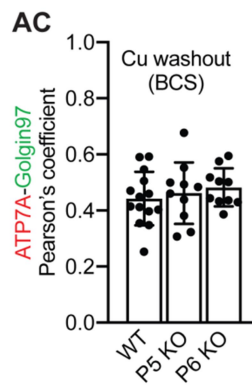
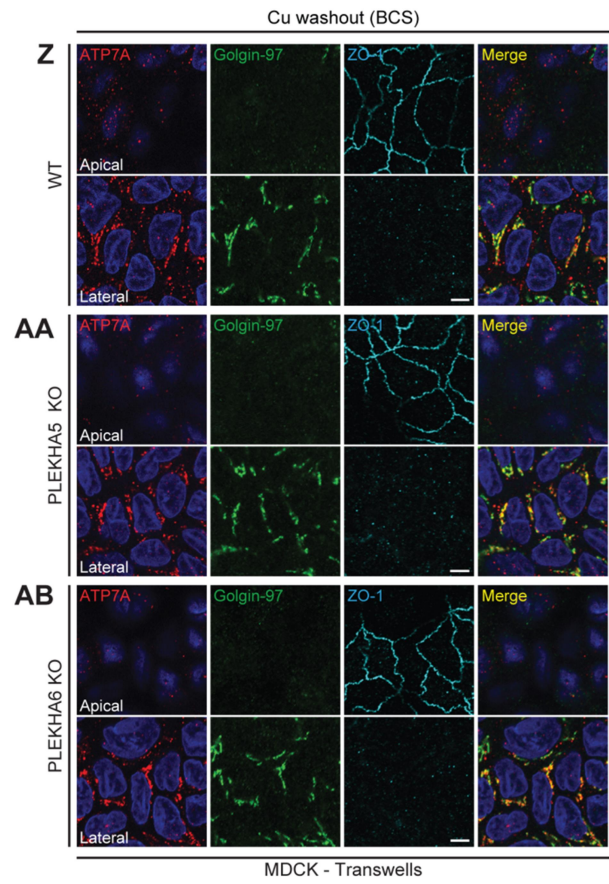
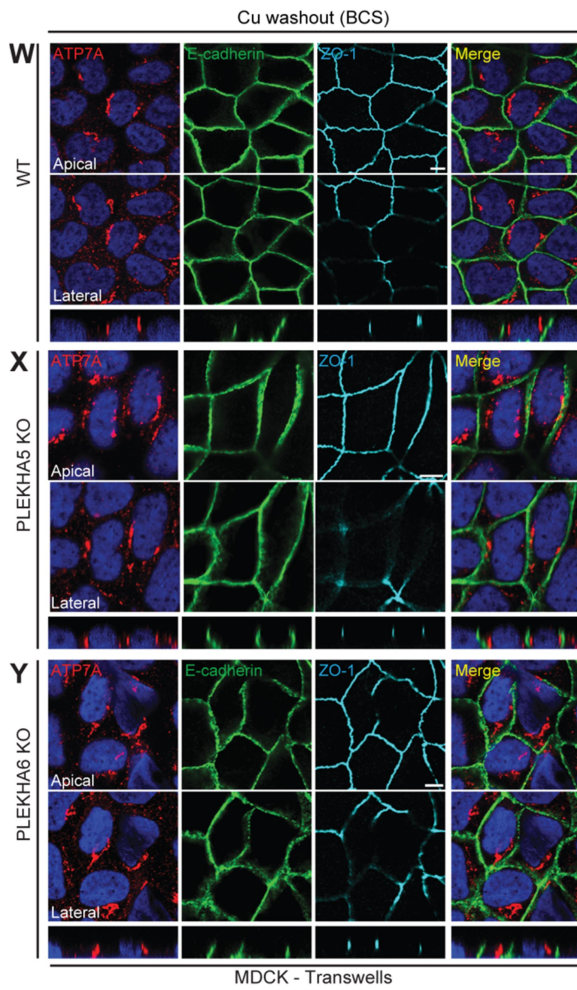


Figure S7-4

Figure S7. Effect of KO of either PLEKHA5 or PLEKHA6 on the localization of ATP7A in polarized MDCK cells. (A-E) IF microscopy analysis of the localization either of ATP7A (red) and TGN marker golgin-97 (green) (A-B) or of ATP7A and apical membrane marker GP135 (C-D), or of ATP7A and early endosome marker EEA1 (E) in MDCK cysts either under Basal Cu (A, C), or elevated Cu (B, D, E). Arrows indicate TGN, lateral (lat.), sub-apical, basal labeling. Arrowheads indicated low/undetectable labeling. Areas in dashed white squares are shown at higher magnification in bottom panels in (E). Bars= 20 μm . (F-K) IF microscopy analysis of the localization of ATP7A in polarized monolayers of MDCK cells (F, I=WT; G, J=PLEKHA5-KO; H, K=PLEKHA6-KO) grown on Transwells under basal (F-H) or elevated (I-K) copper conditions. Dotted white squares/rectangles indicate high magnification areas shown in Figure 4. Bars= 5 μm . (L-Q) IF microscopy analysis of the localization of ATP7A and golgin-97 in polarized monolayers of MDCK cells (L, O=WT; M, P=PLEKHA5-KO; N, Q=PLEKHA6-KO) grown on Transwells under basal (L-N) or elevated (O-Q) copper conditions. Bars= 5 μm . (R-S) Quantification of the colocalization of ATP7A and golgin-97 using Pearson's correlation coefficient under either basal Cu (R) or elevated Cu (S). Dots show replicates corresponding to individual images from 3 independent experiments (n=8-13). Bars represent mean \pm SD and show no significant difference between WT and KO cells. (T-V) IF microscopy analysis of the localization of ATP7A (red) and early endosome marker EEA1 (green) in MDCK grown on Transwells under elevated Cu. Areas in dashed white squares are shown at higher magnification in panels on the right. Bars= 20 μm . (W-Y) IF microscopy analysis of the localization of ATP7A in polarized monolayers of MDCK cells (W=WT; X=PLEKHA5-KO; Y=PLEKHA6-KO) grown on Transwells treated with CuCl_2 before copper washout (chelation with BCS). Bars= 5 μm . (Z-AB) IF microscopy analysis of the localization of ATP7A (red) and TGN marker golgin-97 (green) in MDCK cells (Z=WT, AA= PLEKHA5 KO, AB=PLEKHA6 KO) grown on Transwells treated with CuCl_2 before copper washout (chelation with BCS). Bars= 5 μm . (AC) Quantification of the colocalization of ATP7A and golgin-97 using Pearson's correlation coefficient. Dots show replicates corresponding to individual images from 3 independent experiments (n=10-14). Bars represent mean \pm SD and show no significant difference between WT and KO cells. For XY analysis (F-Q, T-AB), a more apical and a more basal plane of focus were imaged, using ZO-1 and E-cadherin as markers for apical junctions and lateral contacts, respectively. Merge images show colocalization between E-cadherin and ATP7A (F-K, W-Y) or golgin-97 and ATP7A (L-Q, Z-AB) or EEA1 and ATP7A (T-V). ATP7A labeling is detected in the TGN in all cells in basal Cu conditions and is targeted to different degrees to the cell periphery in cells KO for either PLEKHA5 or PLEKHA6. Copper washout resulted in the return of ATP7A to the Golgi in all cells.

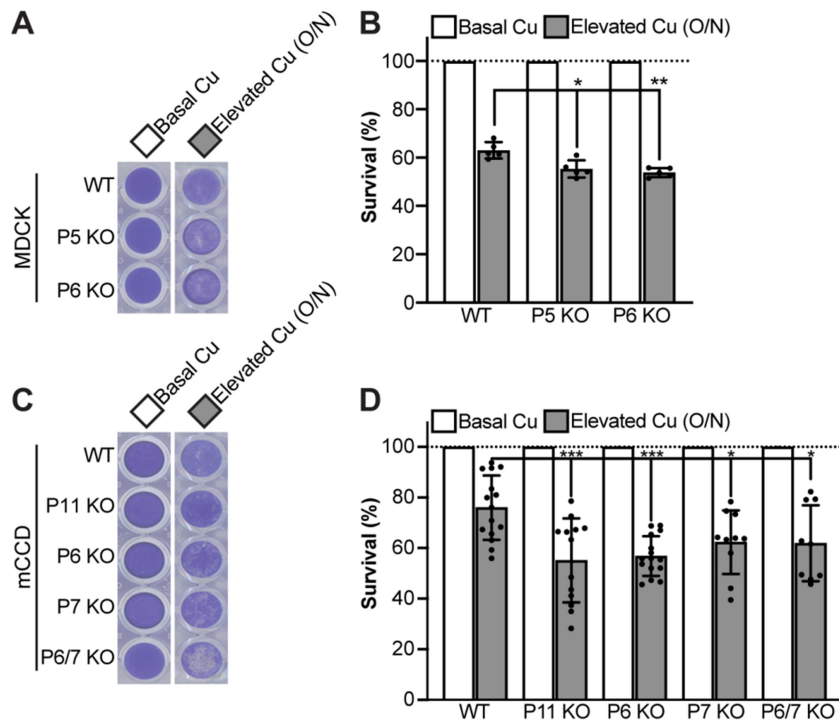


Figure S8

Figure S8. PDZD11 and WW-PLEKHAs are required for cell survival under elevated copper conditions. (A, C) Images of cell culture wells after staining with crystal violet of the indicated WT and KO MDCK (A) and mCCD (C) cells under basal copper (left columns) and elevated copper (right column) conditions. (B, D) Quantification of cell survival, based on crystal violet assay, of each clonal line, either under basal (white columns) or elevated (grey columns) copper. Absorbances are normalized to the basal copper level condition of the corresponding genotype. Dots show replicates ($n=4$ in B, $n=9-15$ in D) and bars represent mean \pm SD. One-way ANOVA with post hoc Dunnett's test ($*p<0.05$, $**p<0.01$, $***p<0.001$). Abbreviations for genotypes: P11=PDZD11; P5=PLEKHA5, P6=PLEKHA6; P7=PLEKHA7.

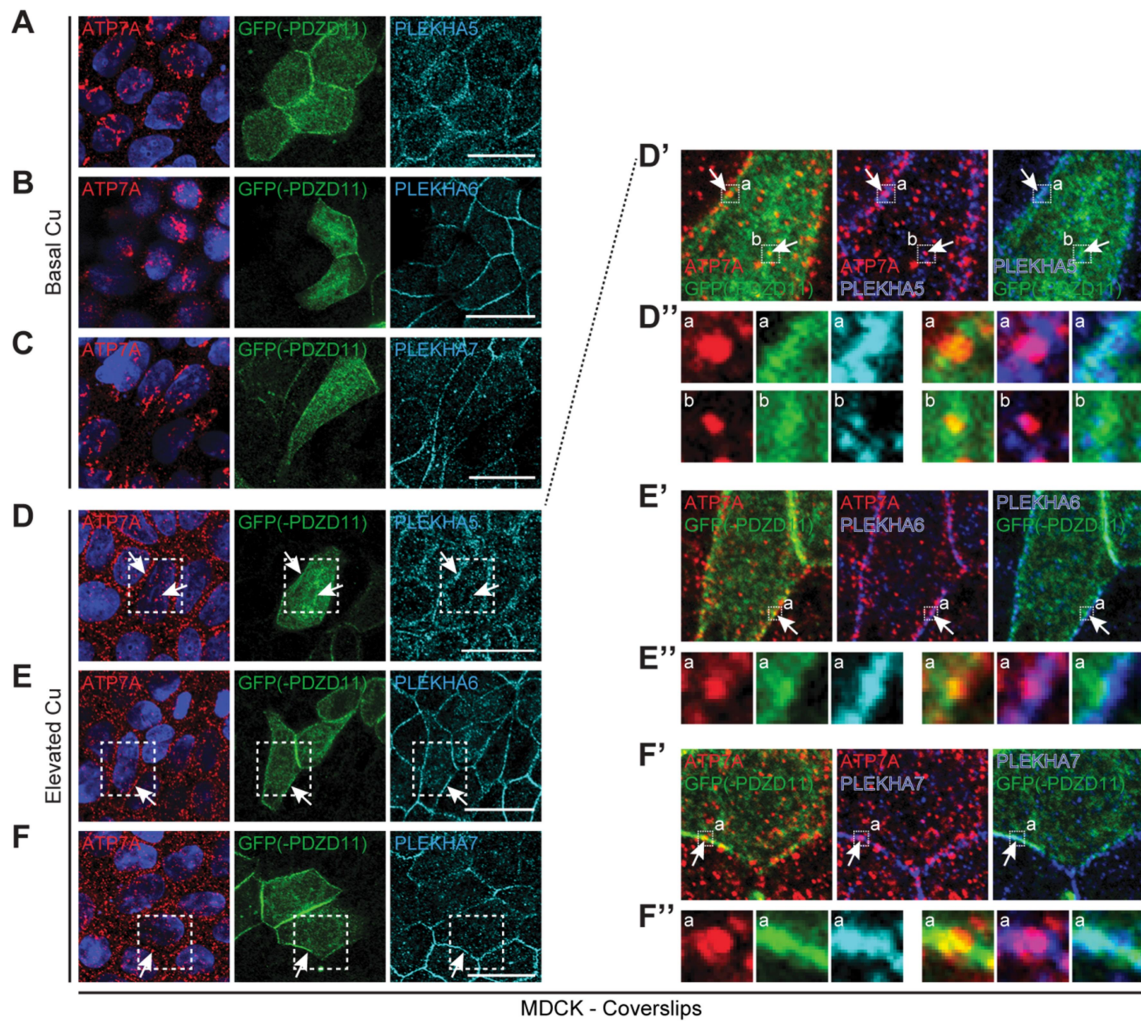


Figure S9

Figure S9. ATP7A, PDZD11 and WW-PLEKHAs colocalize in elevated copper conditions. (A-F) IF microscopy analysis of the localization of endogenous ATP7A (red) and WW-PLEKHAs (cyan) and of exogenous GFP-tagged PDZD11 (green) in MDCK cells grown on glass coverslips, under basal (A-C) or elevated (D-F) copper conditions. (D'-F') are enlarged merged images of dashed squares indicated in (D-F) (WW-PLEKHAs in blue). (D''-F'') are enlarged images of dashed squares indicated in (D'-F'). Arrows indicate labeling, arrowheads indicate low/undetectable labeling. Bars= 20 μm (A-F).

Supplementary Table 1. Summary of localization of WW-PLEKHAs and PDZD11 in cultured cells and tissues.

	PLEKHA5	PLEKHA6	PLEKHA7	PDZD11
mCCD cells	<i>Not detected</i>	Apical AJ and lateral contacts	Apical AJ	Apical AJ (endog.) Apical AJ, lateral contacts and cytoplasm (exog.)
MDCK cells	Lateral contacts and microtubules (also sub-apical in cysts)	Apical AJ and lateral contacts	Apical AJ	AJ
Hap1 cells	AJ and cytoplasm	<i>Not detected</i>	AJ	AJ (Shah <i>et al.</i> , 2018)
bEnd. endothelial cells	AJ (weak) and cytoplasm (exog.)	AJ and cytoplasm (weak) (exog.)	AJ	<i>Not determined</i>
Kidney cortex	Glomeruli Apical and basal surface epithelial cells	Basal surface epithelial cells	Apical AJ epithelial cells	<i>Not determined</i>
Duodenum	Sub-apical cytoplasm of epithelial cells	Apical AJ and basolateral surface epithelial cells	Apical AJ epithelial cells	<i>Not determined</i>
Brain tissue	Endothelial cells Neurons/glia cytoplasmic	Neurons/glia perinuclear	Endothelial cells Neurons/glia cytoplasmic	Neurons/glia perinuclear
Locus coeruleus	Neurons/glia cytoplasmic	Neurons/glia cytoplasmic	Neurons/glia cytoplasmic	Neurons/glia perinuclear
Cortical neurons (primary cultures)	Cytoplasm and neuronal projections	Cytoplasm and neuronal projections	Cytoplasm and nucleus	<i>Not determined</i>

Based on data shown in Figure 2 and Figure S3.

SUPPLEMENTARY KEY RESOURCES TABLE

REAGENT or RESOURCE	SOURCE	IDENTIFIER
Antibodies		
Rabbit polyclonal anti-PLEKHA7	Citi Laboratory (Pulimeno <i>et al.</i> , 2010)	Rb30388
Rabbit polyclonal anti-PDZD11	Citi Laboratory (Guerrera <i>et al.</i> , 2016)	Rb29958
Guinea pig polyclonal anti-PLEKHA7	Citi Laboratory (Guerrera <i>et al.</i> , 2016)	GP2737
Mouse monoclonal anti- β -tubulin	Thermo Fisher Scientific	Cat# 32-2600, RRID: AB_2533072
Mouse monoclonal anti- α -tubulin	Thermo Fisher Scientific	Cat# 32-2500, RRID: AB_2533071
Guinea pig monoclonal anti- α -tubulin	Geneva Antibody Facility (Guerreiro and Meraldi, 2019)	AA345 scFv-F2C
Rabbit polyclonal anti-GFP	Thermo Fisher Scientific	Cat# A-11122, RRID: AB_221569
Mouse monoclonal anti-GFP	Roche	Cat# 11814460001, RRID: AB_390913
Mouse monoclonal anti-HA	Thermo Fisher Scientific	Cat# 32-6700, RRID: AB_2533092
Rabbit polyclonal anti-HA	Santa Cruz Biotechnology	Cat# sc-805, RRID: AB_631618
Mouse monoclonal anti-myc	Citi Laboratory	9E10
Mouse monoclonal anti-E-cadherin	BD Biosciences	Cat# 610181, RRID: AB_397580
Mouse monoclonal anti-ZO-1	Thermo Fisher Scientific	Cat# 33-9100, RRID: AB_2533147
Rat monoclonal anti-ZO-1	Goodenough Laboratory (Harvard Medical School)	R40.76 RRID: AB_2205518
Rabbit polyclonal anti-afadin	Sigma-Aldrich	Cat# A0224, RRID: AB_257871
Rabbit polyclonal anti-paracingulin	Citi Laboratory (Pulimeno <i>et al.</i> , 2011)	20893
Rabbit polyclonal anti-paracingulin	Citi Laboratory (Guillemot <i>et al.</i> , 2008)	n.821
Rabbit polyclonal anti-cingulin	Citi Laboratory (Cardellini <i>et al.</i> , 1996)	C532
Mouse monoclonal anti-p120catenin	Reynolds Laboratory (Wu <i>et al.</i> , 1998)	8D11
Rabbit polyclonal anti- α -catenin	Sigma-Aldrich	Cat# C2081, RRID: AB_476830
Rabbit polyclonal anti- β -catenin	Sigma-Aldrich	Cat# C2206, RRID: AB_476831
Rat monoclonal anti-nectin-3	MBL	Cat# D084-3, RRID: AB_592587
Mouse monoclonal anti-GP135	DSHB	Cat# 3F2/D8, RRID: AB_2618385
Rabbit polyclonal anti-ADAM10	Merck Millipore	Cat# AB19026, RRID: AB_2242320

Mouse monoclonal anti-actin	Merck Millipore	Cat# MAB1501R, RRID: AB_2223041
Mouse monoclonal anti-GFAP	Sigma-Aldrich	Cat# G3893, RRID: AB_477010
Chicken polyclonal anti-GFAP	Invitrogen/Thermo Fisher Scientific	Cat# 01-670-261 RRID: AB_1074620
Mouse monoclonal anti-tubulin β -III	BioLegend	Cat# 801201, RRID: AB_2313773
Rabbit polyclonal anti-ATP7A	Eipper Laboratory (Steveson <i>et al.</i> , 2003)	RbCT78
Mouse monoclonal anti-ATP7A	Santa Cruz Biotechnology	Cat# sc-376467, RRID: AB_1115048
Rat polyclonal anti-PLEKHA5	Citi Laboratory (This paper)	RtSZR129
Rat polyclonal anti-PLEKHA6	Citi Laboratory (This paper)	RtSZR127
Armenian hamster monoclonal anti-PECAM-1	Merck Millipore	Cat# MAB1398Z, RRID: AB_94207
Goat polyclonal anti-VE-cadherin	Santa Cruz Biotechnology	Cat# sc-6458, RRID: AB_2077955
Mouse monoclonal anti-Golgin97	Thermo Fisher Scientific	Cat# A-21270, RRID: AB_221447
Mouse monoclonal anti-EEA1	BD Biosciences	Cat# 610457, RRID: AB_397830
Alexa Fluor 488-AffiniPure Donkey anti-Rabbit IgG	Jackson ImmunoResearch	Cat# 711-545-152, RRID: AB_2313584
Alexa Fluor 488-AffiniPure Donkey anti-Mouse IgG	Jackson ImmunoResearch	Cat# 715-546-151, RRID: AB_2340850
Alexa Fluor 488-AffiniPure Donkey anti-Rat IgG	Jackson ImmunoResearch	Cat# 712-546-153, RRID: AB_2340686
Alexa Fluor 488-AffiniPure Donkey anti-Guinea Pig IgG	Jackson ImmunoResearch	Cat# 706-546-148, RRID: AB_2340473
Cy3-AffiniPure Donkey anti-Rabbit IgG	Jackson ImmunoResearch	Cat# 711-165-152, RRID: AB_2307443
Cy3-AffiniPure Donkey anti-Mouse IgG	Jackson ImmunoResearch	Cat# 715-165-151, RRID: AB_2315777
Cy3-AffiniPure Donkey anti-Rat IgG	Jackson ImmunoResearch	Cat# 712-166-153, RRID: AB_2340669
Alexa Fluor 647-AffiniPure Donkey anti-Guinea Pig IgG	Jackson ImmunoResearch	Cat# 706-605-148, RRID: AB_2340476
Alexa Fluor 647-AffiniPure Donkey anti-Rabbit	Jackson ImmunoResearch	Cat# 711-605-152, RRID: AB_2492288
Alexa Fluor 647-AffiniPure Donkey anti-Goat	Jackson ImmunoResearch	Cat# 705-606-147, RRID: AB_2340438
Cy5-AffiniPure Donkey anti-Rat IgG	Jackson ImmunoResearch	Cat# 712-175-153, RRID: AB_2340672
Cy5-AffiniPure Donkey anti-Mouse IgG	Jackson ImmunoResearch	Cat# 715-605-151, RRID: AB_2340863
DyLightTM405-AffiniPure Goat Anti-Armenian Hamster IgG	Jackson ImmunoResearch	Cat# 127-475-160 RRID: AB_2338994
Alexa Fluor Plus 555-Highly Cross-Adsorbed Goat anti-Mouse IgG	Thermo Fisher Scientific	Cat# A32727 RRID: AB_2633276
Alexa Fluor Plus 488-Cross-Adsorbed Goat anti-Chicken IgY	Thermo Fisher Scientific	Cat# A32931 RRID: AB_2762843

Anti-Mouse IgG (H+L), HRP conjugate	Promega	Cat# W4021, RRID: AB_430834
Anti-Rabbit IgG (H+L), HRP conjugate	Promega	Cat# W4011, RRID: AB_430833
Anti-Rat IgG (H+L), HRP conjugate	Thermo Fisher Scientific	Cat# 62-9520, RRID: AB_2533965
Bacterial Strains		
BL21-DE3 Competent cells	NEB	Cat# C2530H
DH5- α Competent cells	Thermo Fisher Scientific	Cat# 18265017
Chemicals and Recombinant Proteins		
Matrigel	BD Biosciences	Cat# 354230
Poly-D-lysine solution	Thermo Fisher Scientific	Cat# A3890401
Poly-L-Lysine solution	Sigma-Aldrich	Cat# P4707
Cytosine arabinoside (AraC)	Brunschwig	Cat# CAY16069
Nocodazole Ready Made Solution 5 mg/mL, DMSO solution	Sigma-Aldrich	Cat# SML1665
Cupric chloride dihydrate – suitable for cell culture	Sigma-Aldrich	C3279
Bathocuproinedisulfonic acid disodium salt	Santa Cruz Biotechnology	Sc-217698
Copper Fluor-4 (CF4) probe	(Xiao <i>et al.</i> , 2018)	N/A
Control Copper Fluor-4 Sulfur 2 (Ctrl-CF4-S2) probe	(Xiao <i>et al.</i> , 2018)	N/A
Trace-metals grade concentrated nitric acid	VWR (Normatom)	Cat# 83872.290
ICP standard mono-element solution of rhodium	SCP Science	Cat# 140-052-450
ICP standard mono-element solution of copper	SCP Science	Cat# 140-051-290
GST-human PDZD11	Citi Laboratory (Guerrera <i>et al.</i> , 2016)	S1743
GST-human PDZD11-Nter. (1-30)	Citi Laboratory (Rouaud <i>et al.</i> , 2020)	S2034
GST-human PDZD11- Δ 24 (25-140)	Citi Laboratory (Rouaud <i>et al.</i> , 2020)	S2032
GST- human PLEKHA7-WW (1-162)	Citi Laboratory (Guerrera <i>et al.</i> , 2016)	S1792
GST-human PLEKHA5-WW (1-120)	Citi Laboratory (This paper)	S2084
GST-human PLEKHA5-Cter (817-1116)	Citi Laboratory (This paper)	S2085
GST-human PLEKHA6-WW (1-116)	Citi Laboratory (This paper)	S2086
GST-human PLEKHA6-Cter (971-1297)	Citi Laboratory (This paper)	S2087
Critical Commercial Assays		
DNeasy Blood and Tissue kit	QIAGEN	Cat# 69504
Lipofectamine 2000	Invitrogen	Cat# 11668027
jetOPTIMUS DNA Transfection Reagent	Polyplus	Cat# 117-15
Polyethylenimine, Linear, MW 25000	Polysciences	Cat# 23966-2
Pierce Glutathione Magnetic Agarose Beads	Thermo Fisher Scientific	Cat# 78602
Pierce Cell Surface Protein Isolation Kit	Thermo Fisher Scientific	Cat# 89881
Dynabeads protein G for Immunoprecipitation	Thermo Fisher Scientific	Cat# 1004D
Dynabeads protein A for Immunoprecipitation	Thermo Fisher Scientific	Cat# 1001D
Protease inhibitor cocktail	Thermo Fisher Scientific	Cat# A32965
Protease and phosphatase inhibitor cocktail	Thermo Fisher Scientific	Cat# A32959
NucleoSpin RNA Purification Kit	Macherey-Nagel	Cat# 740955.50

iScript cDNA Synthesis Kit	Bio-Rad	Cat# 1708891
SYBR Select Master Mix for CFX	Thermo Fisher Scientific (Life Technologies)	Cat# 4472942
Deposited Data		
GTEEx Analysis Release V8 - dbGaP Accession phs000424.v8.p2	GTEEx portal	gtexportal.org/home/
Experimental Models: Cell Lines		
Mouse cortical collecting duct cell line, mCCD WT N64-Tet-ON	Feraille Laboratory, Unige	N/A
Mouse cortical collecting duct cell line, mCCD PLEKHA7-KO N64-Tet-ON	Citi Laboratory (Shah <i>et al.</i> , 2016; Shah <i>et al.</i> , 2018)	N/A
Mouse cortical collecting duct cell line, mCCD PDZD11-KO N64-Tet-ON	Citi Laboratory (Guerrera <i>et al.</i> , 2016)	N/A
Mouse cortical collecting duct cell line, mCCD PLEKHA6-KO N64-Tet-ON	Citi Laboratory (This paper)	N/A
Mouse cortical collecting duct cell line, mCCD PLEKHA6/7-KO N64-Tet-ON	Citi Laboratory (This paper)	N/A
Canine kidney proximal tubule cell line, MDCK-II WT Tet-OFF	Fanning Laboratory, U. North Carolina	N/A
Canine kidney proximal tubule cell line, MDCK-II PLEKHA5-KO Tet-OFF	Citi Laboratory (This paper)	N/A
Canine kidney proximal tubule cell line, MDCK-II PLEKHA6-KO Tet-OFF	Citi Laboratory (This paper)	N/A
Human haploid cell lines, Hap1 WT, PLEKHA7-KO	Amieva Laboratory, Standford (Popov <i>et al.</i> , 2015)	N/A
Human haploid cell line, Hap1 PDZD11-KO	Citi Laboratory (Shah <i>et al.</i> , 2018)	N/A
Human haploid cell line, Hap1 PLEKHA5-KO	Citi Laboratory (This paper)	N/A
Human haploid cell line, Hap1 PLEKHA5/7-KO	Citi Laboratory (This paper)	N/A
Mouse ciliated embryonic aorta-derived endothelial cell line, meEC	Kwak Laboratory, Unige	N/A
Mouse brain microvascular endothelial (endothelioma) cell line, bEnd.3	Imhof Laboratory, Unige	N/A
Human umbilical vascular endothelial cells, HUVEC	Imhof Laboratory, Unige	N/A
Mouse heart endothelial cell line, H5V	Lampugnani Laboratory, IFOM,	N/A
Human lung carcinoma cell line, A427	Paggi Laboratory, Regina Elena NCI	N/A
Human embryonic kidney, HEK293T	ATCC	N/A
Mouse mammary epithelial cell line, Eph4	Reichmann Laboratory, Hebrew University of Jerusalem	N/A
Human intestinal carcinoma cell line, Caco-2 BBE	Dr. Wangsun Choi, Harvard Medical School	N/A
Human keratinocyte cell line, HaCaT	Fontao Laboratory, Unige	N/A
Oligonucleotides		
CRISPR targets sequences: mouse PLEKHA6 GGTTCATAGAGCTTTTGCGC GCCAGTCTTTATGACGAGC	This paper	N/A

Genotyping primers: mouse PLEKHA6 gaggaattcCCAAGTTACCCCGAGAAGGG gagaagcttGGGAGGAGAGGACGTACCAT	This paper	N/A
CRISPR target sequence: human PLEKHA5 AATGCACCGGTTGTACAGACG	This paper	N/A
Genotyping primers: human PLEKHA5 CAGGTAGGACAAAATACTGCCAC CTGAAACCTAGCTGCAAACCTGG	This paper	N/A
CRISPR target sequence: dog PLEKHA5 TGGACTTACGGGATCACCCG	This paper	N/A
CRISPR target sequence: dog PLEKHA6 CCACCCGAATGTTGATGAGC	This paper	N/A
Genotyping primers: dog PLEKHA6 gaggaattcAAGCTGCTGGGCAAATTGTGTGA gagaagcttCCAGAACTACCGTCCAAGCAGCC	This paper	N/A
qPCR mouse metallothionein-I Fw: GAATGGACCCCAACTGCTC Rv: GCAGCAGCTCTTCTTGACG	(Wunderlich <i>et al.</i> , 2010)	N/A
qPCR mouse GAPDH Fw: GTGCAGTGCCAGCCTCGTCC Rv: CTCGGCCTTGACTGTGCCGT	Citi Laboratory (This paper)	N/A
Recombinant DNA		
pcDNA3.1(zeo+) human PDZD11-HA	Citi Laboratory (Guerrera <i>et al.</i> , 2016)	S1766
pcDNA3.1(zeo+) GFP-human PDZD11-myc	Citi Laboratory (Guerrera <i>et al.</i> , 2016)	S1744
pTRE2hyg YFP-human PLEKHA7-myc	Citi Laboratory (Paschoud <i>et al.</i> , 2014)	S1431
pTRE2hyg YFP-human PLEKHA7-Nter (1-562)-myc	Citi Laboratory (Paschoud <i>et al.</i> , 2014)	S1432
pEGFP-N3 human Tspan15	Citi Laboratory (Shah <i>et al.</i> , 2018)	S2152
pEGFP-N1 human Tspan33	Citi Laboratory (Shah <i>et al.</i> , 2018)	S2154
pcDNA3.1(zeo+) CFP-HA	Citi Laboratory (Guerrera <i>et al.</i> , 2016)	S1150
pcDNA3.1(-) GFP-myc	Citi Laboratory (Paschoud <i>et al.</i> , 2011)	S1166
pTRE2hyg YFP-myc	Citi Laboratory (Paschoud <i>et al.</i> , 2014)	S1210
pTRE2hyg YFP-human PLEKHA5-myc	Citi Laboratory (This paper)	S2082
pTRE2hyg YFP-human PLEKHA6-myc	Citi Laboratory (This paper)	S2083
pcDNA3.1(-) GFP-human PLEKHA5	Citi Laboratory (This paper)	S2530
pcDNA3.1(-) GFP-human PLEKHA6	Citi Laboratory (This paper)	S2531
pcDNA3.1(-) HA-human PLEKHA5	Citi Laboratory (This paper)	S2567
pcDNA3.1(-) HA-human PLEKHA6	Citi Laboratory (This paper)	S2568
pcDNA3.1(-) HA-human PLEKHA7 Nter (1-562)	Citi Laboratory (This paper)	S2589

pcDNA3.1(-) GFP-human ATP7A-Cter WT (1462-1500)	Citi Laboratory (This paper)	S2698
pcDNA3.1(-) GFP-human ATP7A-Cter Δ PDZ-binding (1462-1496)	Citi Laboratory (This paper)	S2699
pSpCas9(BB)-2A-GFP (px458)	(Ran <i>et al.</i> , 2013)	Addgene #48138
Softwares and Algorithms		
FIJI	NIH	RRID: SCR_002285
Adobe Photoshop	Adobe	RRID: SCR_014199
Adobe Illustrator	Adobe	RRID: SCR_010279
T-Coffee (version 8.93)	EMBL-EBI	RRID: SCR_011818
NCoils (version 1)	Expasy_Embnet	RRID: SCR_008440
PROSITE	Expasy	RRID: SCR_003457
WebLogo 3.7.4	weblogo.threeplusone.com/	RRID: SCR_010236
Image Studio Lite	LI-COR	RRID: SCR_013715
SnapGene	N/A	RRID: SCR_015052
Prism 8	GraphPad	RRID: SCR_002798